Large Ca isotope effect in the CaC_6 superconductor

D. G. Hinks, D. Rosenmann, H. Claus, M. S. Bailey, and J. D. Jorgensen
Materials Science Division, Argonne National Laboratory, Argonne, Illinois 60439, USA
(Received 6 November 2006; published 9 January 2007)

We have measured the Ca isotope effect coefficient, α(Ca), in the newly discovered superconductor CaC_6 and find a value of 0.53(2). This result shows that the superconductivity is dominated by coupling of the electrons by Ca phonon modes. The C phonons contribute very little, assuming that this material is a conventional electron-phonon coupled superconductor. Thus, in contrast to another layered material MgB_2, where high-energy phonons in the B layers are responsible for the superconductivity, in layered CaC_6 the phonons responsible for superconductivity are primarily low-energy modes of the intercalated Ca.

DOI: 10.1103/PhysRevB.75.014509 PACS number(s): 74.62.−c, 74.25.Kc, 74.70.Ad

INTRODUCTION

The recent discovery of superconductivity[1,2] at 11.5 K in a Ca graphite intercalation compound (GIC) has renewed interest in the superconducting behavior of this class of materials. Superconductivity in the alkali GICs was first reported in 1965;[3] however, T_cs were well below 1 K. The low T_cs, the reactivity to air, difficult synthesis, and irreproducible superconducting transitions have been impediments to many workers. As an example, the original T_c reported by Hannay *et al.*[3] was 390 mK for KC_8; however, initial attempts to reproduce this result were elusive. Poitrenaud[4] could find no evidence for superconductivity down to 300 mK. A flurry of activity around 1980[5–7] showed that the T_c of the KC_8 compound was much lower and could vary over a considerable temperature range (128–198 mK) depending on synthesis conditions.[7]

The first synthesis of CaC_6 was performed by Weller *et al.*[1] using Ca vapor transport. These samples were not homogeneous and the resulting superconducting transitions were broad. Emery *et al.*[2] was able to synthesize bulk samples (at least 60% phase fraction) with sharp transitions using a Li-Ca alloy. Highly oriented pyrolytic graphite (HOPG) was immersed in a Li-Ca solution (75 at. % Li) at approximately 350 °C for several days. Li is initially intercalated into the HOPG followed by a slow exchange of Ca for Li.[8] Using lower temperatures and different Li-Ca flux compositions, ternary Li-Ca-C compounds can also be obtained.[9,10] One of these materials, $Li_3Ca_2C_6$, was shown to have a superconducting onset at 11.15 K,[10] approximately 0.35 K less than the binary CaC_6. The hypothesis concerning $Li_3Ca_2C_6$is that the Li and Ca intercalate into separate layers and that the superconductivity comes from the domains intercalated with Ca.

Superconductivity in GICs has a long history and is still an area with some uncertainty. A graphene layer, by itself, is a zero-band-gap semiconductor with the fully occupied π band just touching the unoccupied π^* band at one point in the Brillouin zone. The graphene layers stack to form hexagonal graphite, and the interactions between the layers lead to electron and hole pockets. Graphite is thus a semimetal with an in-plane conductivity much larger than that along the c axis. In all the donor GICs (alkali metals, alkaline earth metals, rare earths, etc.) electrons are transferred from the donor atom to the graphene antibonding π^* bands.[11] This leads to an increase in conductivity of the graphene layers and a reduction in the anisotropy of the conductivity. Likewise, the anisotropy of the superconducting properties is smaller than a simple filling of the π^* band would suggest.

Al-Jishi in 1983 formulated a two-band model for superconductivity in order to explain the reduced anisotropy in the superconducting GICs.[12,13] Two types of bands were postulated to be important for superconductivity, the two-dimensional (2D) π bands and the three-dimensional (3D) intercalate band. This intercalate band, also called the "alkali band", was formed from the s orbitals of the intercalate ion and is partially occupied since charge transfer from the alkali to the π^* band is incomplete. In this model, superconductivity results from the coupling between electrons on the 2D π bands and the 3D intercalate band, leading to a reduction in the anisotropy. The nature of this 3D band has been the subject of some controversy. At about the same time, Posternak *et al.*[14] in their calculations on model 2D systems, observed a previously unknown band in pure graphite. This 3D "electron-like" interlayer band was formed from interlayer states in the graphite and was located far above the Fermi level. The interaction of this band with the intercalate orbitals was predicated to lead to the alkali or intercalate band. Recently Csányi *et al.*[15] investigated this interlayer band in detail and showed that its presence at the Fermi level is a predictor of superconductivity.

However, the nature of the pairing mechanism in the GICs is still not fully understood. In general, the coupling of the phonon modes of the graphene layers to the π bands is weak with no coupling of the out-of-plane lattice modes and only weak coupling of the in plane modes. Assuming T_c is determined by C phonons, the low T_cs of these materials might be expected based on the small coupling to the electrons. The appearance of the high T_c in CaC_6 was thus surprising. Csányi *et al.*[15] suggests that an electronic mechanism may be responsible for the high T_c. Mazin,[16] on the other hand, suggests most of the coupling is due to Ca phonons. He assumed that the difference in T_c between CaC_6 and YbC_6 is due mainly to the difference in mass of the intercalated ions. Based on this idea, he predicts a Ca isotope effect coefficient (IEC) of about 0.4 where the IEC (α) is defined as

$$\alpha = -d \ln T_c / d \ln M.$$

Calandra and Mauri,[17] using density functional theory, calculated that the Ca in-plane and C out-of-plane vibrations me-

diate the superconductivity somewhat equally, with small contributions from other vibrations. Their calculated Ca and C isotope effect coefficients are 0.24 and 0.26, respectively.

Thus, a measurement of the Ca isotope effect could help in determining the contribution of the Ca phonon modes to superconductivity and as a stringent test of any theoretical calculations. Normally for *sp* materials the canonical value of α is 0.5, whereas *d*-electron systems usually show a reduced isotope effect coefficient.[18] For a multicomponent system the sum over the individual isotope effect coefficients should have a maximum value of 0.5. The isotope effect coefficient has not been measured for any GIC to date, probably due to the low T_cs of the materials and the difficulty in obtaining reproducible superconducting transitions. CaC_6 is a material that shows a narrow, reproducible T_c that is high enough to yield a large ΔT_c for isotopic substitution of either Ca or C. Assuming a full Ca IEC, a ΔT_c of about 0.5 K would be expected between ^{40}Ca and ^{44}Ca. Therefore, this material is an ideal candidate for the isotope effect coefficient measurement.

We have measured the Ca isotope effect coefficient using the ΔT_c between samples made from natural abundance Ca(^{n}Ca) and isotopic ^{44}Ca and, in a second experiment, between ^{40}Ca and the same ^{44}Ca isotope. We find a large isotope effect coefficient for Ca ($\alpha \cong 0.5$), indicating that the entire coupling of electrons in the superconducting state is by Ca phonons, assuming that CaC_6 is a simple BCS superconductor.

EXPERIMENTAL

Magnetization measurements were performed in a noncommercial SQUID magnetometer.[19] The Earth's magnetic field is reduced by a μ-metal shield, yielding a remnant magnetic field of less than 10 mGauss. Magnetic fields up to 50 Gauss can be applied to the sample with a Cu solenoid. The intercalated HOPG samples were contained in a hermetically sealed Ti sample holder to prevent reaction with the ambient atmosphere. The magnetic field was applied perpendicular to the basal plane of the sample during the measurement. Diffraction patterns were taken with a PANalytical X'Pert PRO x-ray diffractometer using Co Kα radiation. The HOPG sample was placed on a rotating stage using Bragg-Brentano geometry to measure *c*-axis reflections.

We have tried both flux intercalation, using 75 at. % Li solutions, and vapor transport to prepare the samples. We find that vapor transport, while not giving fully intercalated samples, yields sharp, reproducible superconducting transitions while avoiding other possible adverse effects that may result when using the Li-Ca alloy melt. The absence of Li in the synthesis procedure negates the possible formation of other Ca-Li intercalation compounds, as described in Ref. 10, and possible solid solutions leading to T_c variation. Li may also introduce other alkali metals into the system that are known to form GICs with lower T_cs. In vapor transport, only impurities that have sufficient vapor pressure can incorporate, whereas in the alloy synthesis, the alloy melt is in direct contact with the HOPG, allowing impurities to possibly incorporate more easily. The high cost of ^{44}Ca is also a factor since a much larger quantity of the isotope is needed for the alloy method than that required for vapor transport, thus limiting the amount of alloy that can be used. If the quantity of alloy is too small, composition changes during intercalation could occur, leading to other phases.

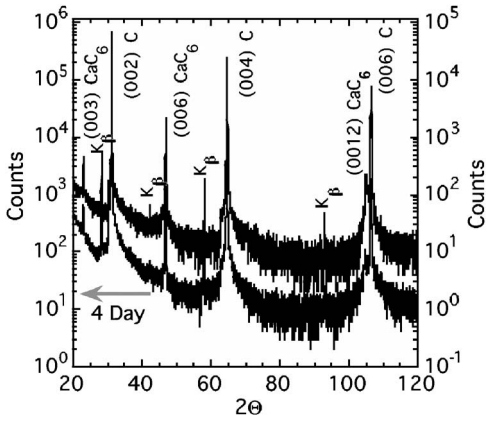

FIG. 1. X-ray diffraction pattern of a 4-day (lower) and a 12-day (upper) vapor-transport-synthesized sample showing both the HOPG and CaC_6 (001) diffraction peaks. The pattern was taken using Co Kα radiation.

The vapor-phase synthesis was done by intercalating GE Advance Ceramics grade ZYA HOPG with a mosaic spread of $0.4° \pm 0.1°$. Samples were cut to a 2×2 mm^2 sample size with thicknesses of about 0.4 mm. All the samples were taken from the same larger $12 \times 12 \times 2$ mm^3 HOPG plate, ensuring the same chemical and physical properties. For each of the two syntheses runs, two isotopic intercalations were fired simultaneously in the furnace. For each of the isotopic intercalations about 60 mg of a Ca isotope along with two or three HOPG samples were placed in a 40 mm long by 9.5 mm diam stainless steel tube. The tube ends were tightly squeezed shut, but not welded, therefore allowing for subsequent evacuation of the tube. The loading of the stainless tubes was done in an N_2-filled glove bag. The stainless tubes were transferred to a vacuum system and pumped to 4×10^{-3} MPa. After 1 day the temperature was raised to 450 °C and the intercalation took place for either 4.2 (the 4-day samples) or 12.1 days (the 12-day samples). Pumping, to remove outgasing products, was continued through the entire intercalation process to keep the pressure in the ampoules low and the mean-free path of the Ca vapor large to ensure good Ca transport. For the 4-day reaction natural abundance Ca (Rare Earth Products, 99.98% purity) and ^{44}Ca (Oak Ridge 98.78% enrichment, calculated atomic weight 43.93) isotopes were used, and for the 12-day synthesis^{40}Ca (Oak Ridge 99.97% enrichment, 39.96 calculated atomic weight) and the same ^{44}Ca isotope was employed.

RESULTS

Figure 1 shows the diffraction pattern for both a 4-day and a 12-day intercalated sample. The samples are clearly two phase, consisting of rhombohedral CaC_6 and unintercalated, hexagonal graphite. While the amount of CaC_6 is small, it is adequate to easily measure the superconducting transition temperature by magnetization.

Figure 2 shows the normalized superconducting transitions for the two series of samples. The 4-day and the 12-day intercalated samples are represented by solid and dashed lines, respectively. Superconducting transitions are shown for at least two samples from each ampoule, showing the good reproducibility of the intercalation within an ampoule. The 4-day samples were measured after field cooling in a magnetic field of 1 G (parallel to the *c* axis of the HOPG) to 4.2 K and then the magnetization was recorded on warming in the 1 G field. The 12-day samples were zero-field cooled and measured on warming in 0.1 G. The reason for the different measurement protocol for the 4- and 12-day samples will be discussed later. The 4- and 12-day transitions shown in Fig. 2 cannot be directly compared, since each measurement protocol monitors a different aspect of magnetic flux penetration in the sample. The 4-day field-cooled transitions monitor the reentrance of the flux that was expelled on cooling the sample (usually only a few percent of the total flux). The 12-day zero-field-cooled samples measure the entire flux entrance into the sample. The field-cooled transition may thus appear sharper and (depending on the criteria for determining T_c) at a slightly higher transition temperature than the zero-field-cooled measurement. Figure 2 shows that the normalized magnetizations, the actual magnitude of the Meissner magnetization (zero-field-cooled measurement) at low temperatures range from 4 to 8×10^{-6} emu for the various samples; however, the absolute magnitude has little meaning for these multiphase samples.

The value of the IEC will depend strongly on the criterion for the determination of T_c for the samples. This is important for this experiment, since the measured transitions for the 12-day samples are broader, most likely due to the different measurement protocols employed. The onset T_c should be used to calculate α, since the transition width depends more on the flux pinning properties of the samples than any intrinsic variation in T_c due, for example, to variations in stoichiometry or purity. We have used two different criteria for the onset T_c: (1) the linear extrapolation to zero magnetization of the slope at the inflection point and (2) the temperature at 5% of the normalized transition. Table I shows the transition temperatures determined for the samples using the average of the two or three samples in each synthesis tube. The calculated Ca isotope effect coefficient is also shown for each of the isotopic pairs. The extrapolated and 5% T_cs are, within the experimental accuracy, the same, leading to about the same calculated values of α. The average value over the various determinations is $\alpha=0.53(2)$, with the error determined only by the precision of the temperature determination.

If one looks closely at the data in Fig. 2 and Table I it is apparent that the onset temperatures for the ^{44}Ca 4- and 12-day samples are within the experimental error of 0.01 K. The reproducibility of the measured T_c between these two synthesis runs shows that the vapor phase synthesis is very robust and that the measurement protocol has very little impact on the measured T_cs. In contrast to this, the calculated T_c (assuming α is 0.5) of the 12-day ^{40}Ca should be 15 mK higher than the ^{n}Ca 4-day sample. However, the actual T_c of the ^{40}Ca 12-day sample is lower by about 50 mK. This most likely indicates an impurity effect on T_c, with the ^{n}Ca having

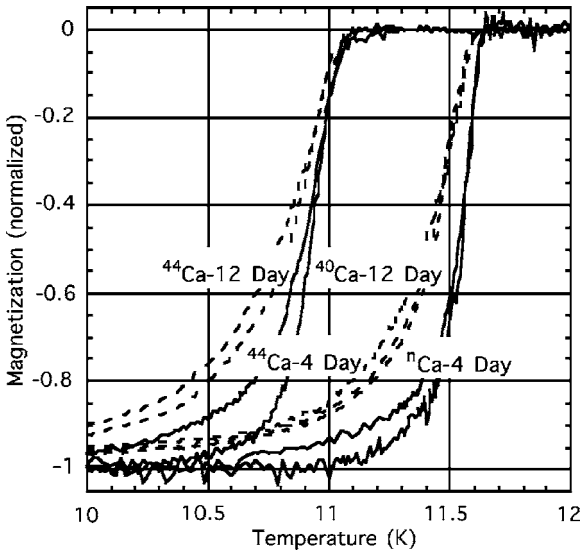

FIG. 2. Normalized magnetization versus temperature for the isotopic Ca-intercalated HOPG. The natural abundance Ca and the ^{44}Ca 4-day samples are shown as solid lines, and the ^{40}Ca and ^{44}Ca12-day intercalated samples are shown as dashed lines. The data for the 4-day samples were taken on warming in 1 G after field cooling in 1 G while the 12-day samples were measured in 0.1 G after zero field cooling.

a much higher purity and thus yielding a higher T_c. Reference 20 lists the impurities reported by the manufactures of the three Ca isotopes employed. The detection limits for the various elements not analytically found (that are not listed in Ref. 20) are also much larger for the Oak Ridge isotopes. Thus, the enriched isotopes may have a larger impurity content that the natural abundance material and this may be responsible for the enhanced T_c of the ^{n}Ca sample. Based on this one might speculate that the 12-day intercalation is a more accurate measurement of α, since we are comparing two similar Ca materials both having been enriched in the same manner. That measurement gives a lower value of α closer to the canonical value of 0.5. However, since the nature of any impurity interactions are not known at present and there is no control over the purity content of the Ca isotopes, we must use the data from both intercalation runs. One must understand that the reported error in α only measures the precision of the experiment and that the accuracy of

TABLE I. The transition temperatures for the various isotopically substituted CaC_6 samples and the calculated isotope effect coefficient, α, for the various experiments. The error in the transition temperature is ±0.01 K. The error in α is determined only by the error in temperature and ignores any other errors, such as impurity effects, that may be present.

Sample	T_c (K) (onset)	α	T_c (K) (at 5%)	α
^{n}Ca-4 day	11.62	0.55(2)	11.62	0.55(2)
^{44}Ca-4 day	11.05		11.05	
^{40}Ca-12 day	11.57	0.50(2)	11.58	0.52(2)
^{44}Ca-12 day	11.04		11.03	

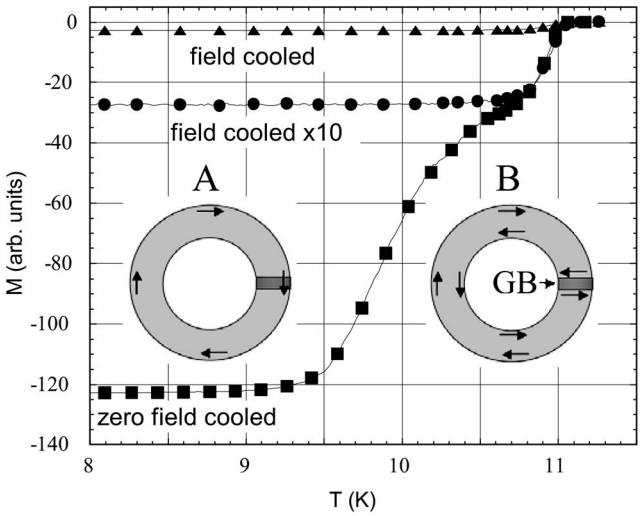

FIG. 3. Field-cooled (in 1 G) and zero-field-cooled magnetization measured in a 1-G field for one of the ^{44}Ca samples (solid triangles in Fig. 1). Also shown are the field-cooled data scaled up by a factor of 10. Inset A shows the shielding current path when the weak link is fully conducting and inset B shows the current path when the weak link becomes insulating (see text).

the experiment (in particular from impurity effects) could be less.

As pointed out previously, the samples are not fully intercalated even after 12 days of heating. The 12-day intercalated samples show sharp superconducting transitions when the zero-field-cooled magnetization is measured as shown in Fig. 2. This is not the case with the 4-day intercalated samples. Figure 3 compares the field-cooled (Meissner) magnetization with the zero-field-cooled (shielding) magnetization for one of the ^{44}Ca, 4-day samples. The magnetic field is 1 G and is parallel to the c axis of the HOPG. The other 4-day intercalated samples show similar behavior, although not as extreme, generally only showing a much-broadened transition for the zero-field-cooled measurement. At first glance it appears that there are two different transitions in this sample but that only the one with a higher T_c displays a Meissner effect. However, this is not the case; instead, the zero-field-cooled magnetization resembles that of a superconducting ring with a weak link.[21]

Ca likely intercalates into the HOPG along the basal planes at the outer surfaces of the HOPG plates. The CaC_6 forms in a ring around the outer surface of the HOPG coupled by weak links with reduced critical currents. The two insets in Fig. 3 demonstrate the schematic current flow in a ring with a single weak link. For the zero-field-cooled state at low temperatures, the induced current is smaller than the critical current of the weak link (inset A). Thus, the induced shielding current at low temperatures flows along the outer perimeter of the sample, yielding a magnetization signal proportional to the area of the entire sample. As the temperature is increased, the critical current of the grain boundary decreases monotonically. Eventually the critical current will drop below the shielding current and the magnetic moment will decrease with increasing temperature as the shielding current is shunted to the inside of the annulus. When the grain boundary critical current reaches zero, which happens

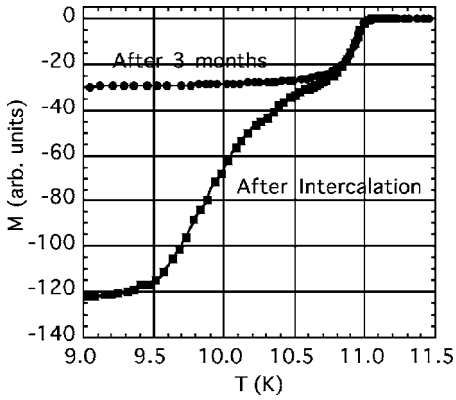

FIG. 4. Zero-field-cooled magnetization measured on warming in a 1-G field for the sample in Fig. 3 after intercalation and after storage for 14 weeks.

at about 10.7 K for the sample in Fig. 3, the current flow is schematically represented by inset B where the current through the grain boundary is zero. The annular ring, however, is still superconducting and will show a transition at T_c with a signal proportional to the area of the superconducting ring. If more than one grain boundary is present, only the weakest one will have an effect on the zero-field-cooled magnetization.[21] Thus, the upper transition measures the true superconducting transition of the CaC_6 and the lower transition is an indirect measure of the weak-link critical current.

This model naturally explains why in the field-cooled magnetization, only the real transition is seen. During cooling of a ring in a field through the superconducting transition, flux will be expelled to the outside of the ring as well as into the bore. The current distribution in the field-cooled state will be essentially the same as in inset B of Fig. 3 (the currents flowing parallel to the grain boundary have no effect in the magnetic moment). Note that this behavior is not present in the 12-day intercalated samples, the field-cooled and zero-field-cooled measurements giving the same transition temperature. The longer intercalation period most likely allowed the Ca to intercalate more uniformly and no weak links appear to have been formed.

The sample shown in Fig. 3 was kept for 14 weeks under N_2 to observe the effect of long-term storage on the transition temperature. Figure 4 shows the zero-field-cooled magnetization measured in a 1-G field after 14 weeks storage compared to the original zero-field-cooled measurement. The magnetization after 14 weeks only shows the upper part of the transition; the weak link behavior is no longer present. At room temperature the Ca must be slightly mobile. As made, the sample contains domains of CaC_6, forming a ring around the sample coupled weakly by either filamentary strands of CaC_6 regions of low T_c, low-Ca CaC_6. Over time the Ca defuses from these weak link regions to the CaC_6 domains, forming isolated regions of CaC_6. The magnetization then only measures the shielding by the superconducting CaC_6 domains. Using this model for the sample, the zero-field-cooled data can give an upper estimate of the superconducting phase fraction. The ratio of the field-cooled magnetization after 14 weeks (assuming all weak links are normal and shielding current only flows around superconducting domains) to the initial field-cooled magnetization (assuming

shielding around the entire sample) will give the phase fraction of superconducting CaC_6. For the sample shown in Fig. 3, this ratio ($\approx 30/120$) will be about 1/4. This would be consistent with a 0.18-mm angular ring around the 2-mm^2 HOPG samples. This, however, is not consistent with the c axis, x-ray diffraction pattern shown in Fig. 1 that indicates a much lower CaC_6 phase fraction, possibly by a factor of 10. These two measurements can be reconciled by assuming that the Ca only intercalates into the HPOG, forming a thin ring around the top and bottom surfaces, possibly due to the large strain introduced during intercalation. Magnetization with the field along the c axis would measure what would appear to be an annular ring over the entire sample thickness, but diffraction would measure the true phase fraction of CaC_6.

DISCUSSION

Our results show that calcium clearly supplies a large phonon contribution to the superconductivity in CaC_6. Considering that this material is an sp system, a maximum value of 0.5 for the total α might be expected. Our measured value for the Ca isotope effect is already at the BCS limit of 0.5, indicating that the contribution to the total IEC by C is zero. However, it may be somewhat unreasonable to expect the C isotope effect coefficient to be negligible. It would be instructive to measure the C isotope effect coefficient to see if the total isotope effect is possibly greater than 0.5. If so, this would then be the second example of a total isotope coefficient greater then 0.5, underdoped high T_C copper oxides being the first.[22] However, the measurement of the carbon isotope effect coefficient is far from trivial since it requires the synthesis of isotopic graphite, a difficult task. Our result indicates that only calcium phonons mediate superconductivity in CaC_6 and that C phonons have, at most, a very small contribution.

Csányi *et al.*[15] pointed out that the 3D interlayer band hybridizes strongly with the π^* bands in the high-T_c CaC_6 and YbC_6 but not in the low-T_c GICs. Thus, electron-phonon coupling of the interlayer band with the metal ion and, through hybridization, with C phonons might be responsible for the high T_c. However, they were unsure if electron-phonon coupling could describe the entire range of T_cs observed in the GICs and suggested that the interlayer state might lead to an excitonic pairing mechanism. Our large value for α(Ca) clearly points to a phonon mechanism.

In general our results are consistent with the suggestion by Mazin[16] that much of the electron-phonon coupling in CaC_6 and YbC_6 was due to the metal-ion phonons. He deduced a large value of 0.4 for the Ca isotope effect coefficient by assuming that the difference in T_c between these two materials is due mostly to the metal-ion mass difference. Although after this suggestion it was found that the two materials have a different stacking sequence, and thus a slightly different electronic structure, his deduction appears correct. We find an even larger value than Mazin for α(Ca).

Calandra and Mauri,[17] using density functional theory, calculated the band structure of CaC_6. They find that the carriers (electrons) are on an intercalate band formed by partial charge transfer from the Ca to the C (about 0.32 electrons/cell). This intercalate band primarily couples to in-plane Ca phonon modes and out-of-plane C modes. The calculated isotope effect coefficients [α(O)=0.24 and α(O)=0.26] are nearly equal and quite different than what we find experimentally. Any coupling of the interlayer or intercalate band to C directly or by hybridization is probably nonexistent since we find only Ca phonons may mediate superconductivity. In this model calculation coupling alone to Ca phonons would not give the high T_c.

Tunneling,[23] specific heat,[24] penetration depth,[25] and resistivity measurements[26] have all led to the conclusion that CaC_6 is a weak to moderately strongly coupled superconductor with a maximum electron-phonon coupling constant of about 0.85. However, the observation of a linear dependence of H_{c2} with temperature[24,26] could be the result of strong electron-phonon coupling. Mazin *et al.*[27] have pointed out that the measurement of α(Ca)=0.5 implies strong coupling, in disagreement with several of the experiments listed above. This is because the energy of the various Ca phonons is low and to obtain the observed T_c of CaC_6 would require strong coupling. More work will be necessary to unambiguously determine the coupling strength in this material.

It is instructive to compare two seemingly similar materials, MgB_2 and CaC_6. Structurally these materials are similar, containing 2D hexagonal nets of B or C separated by an alkaline earth ion. In MgB_2 charge transfer from the Mg to the B network is complete. The interlayer band lies above the Fermi level and is unimportant in this material. It is charge transfer from the B σ bands to the B π bands that creates holes in the σ bands which host the strongest superconducting interaction. These carriers couple strongly to the high-energy, in-plane B vibrations, leading to high-T_C superconductivity. In this material, B shows a large isotope effect (0.30), whereas Mg shows an isotope effect of only 0.02.[28] In CaC_6 charge transfer is not complete, leading to an interlayer (or intercalate) band at the Fermi level. This band couples with the Ca phonons and, according to our result, this interaction is solely responsible for the high T_c. At present the nature of this interlayer (or intercalate) band is somewhat uncertain and the interaction of this band with the Ca phonons to give the observed T_c is still not understood.

This example of the intercalated cations, rather than the 2D graphite layers, being responsible for superconductivity suggests an additional strategy for searching for new superconducting materials. Perhaps one should look for systems where a 2D template can be used to "suspend" or arrange light atoms in such a way that phonon amplitudes are unusually large, owing to longer that normal distances between the cations and giving rise to strong electron-phonon coupling.

ACKNOWLEDGMENTS

This work was supported by the U.S. Department of Energy, Basic Energy Sciences–Materials Sciences, and the Office of Energy Efficiency and Renewable Energy under Contract DE-AC02–06CH11357. We wish to thank Ken Gray for useful discussions about the interpretation of these results.

[1] T. E. Weller, M. Ellerby, S. S. Saxena, R. P. Smith, and N. T. Skipper, Nat. Phys. **1**, 39 (2005).
[2] N. Emery, C. Hérold, M. d'Astuto, V. Garcia, C. Bellin, J. F. Marêché, P. Lagrange, and G. Loupias, Phys. Rev. Lett. **95**, 087003 (2005).
[3] N. B. Hannay, T. H. Geballe, B. T. Matthias, K. Andres, P. Schmidt, and D. MacNair, Phys. Rev. Lett. **14**, 225 (1965).
[4] J. Poitrenaud, Rev. Phys. Appl. **5**, 275 (1970).
[5] Y. Koike, H. Suematsu, K. Higuchi, and S. Tanuma, Solid State Commun. **27**, 623 (1978).
[6] M. Kobayashi and I. Tsujikawa, J. Phys. Soc. Jpn. **46**, 1945 (1979).
[7] Y. Koike, S.-I. Tanuma, H. Suematsu, and K. Higuchi, J. Phys. Chem. Solids **41**, 1111 (1980).
[8] N. Emery, C. Hérold, and P. Lagrange, J. Solid State Chem. **178**, 2947 (2005).
[9] S. Pruvost, P. Berger, C. Hérold, and P. Lagrange, Carbon **42**, 2049 (2004).
[10] N. Emery, C. Hérold, J.-F. Marâché, C. Bellouard, G. Loupias, and P. Lagrange, J. Solid State Chem. **179**, 1289 (2006).
[11] T. Enoki, M. Suzuki, and M. Endo, *Graphite Intercalation Compounds and Applications* (Oxford University Press, Inc., New York, 2003).
[12] R. Al-Jishi, Phys. Rev. B **28**, 112 (1983).
[13] R. A. Jishi and M. S. Dresselhaus, Phys. Rev. B **45**, 12465 (1992).
[14] M. Posternak, A. Baldereschi, A. J. Freeman, E. Wimmer, and M. Weinert, Phys. Rev. Lett. **50**, 761 (1983).
[15] G. Csányi, P. B. Littlewood, A. H. Nevidomskyy, C. J. Pickard, and B. D. Simons, Nat. Phys. **1**, 42 (2005).
[16] I. I. Mazin, Phys. Rev. Lett. **95**, 227001 (2005).
[17] M. Calandra and F. Mauri, Phys. Rev. Lett. **95**, 237002 (2005).
[18] J. W. Garland, Jr., Phys. Rev. Lett. **11**, 114 (1963).
[19] K. Vandervoort, G. Griffith, H. Claus, and G. W. Crabtree, Rev. Sci. Instrum. **62**, 2271 (1991).
[20] The three Ca isotopes do differ in impurity content. The reported impurities in the ^{44}Ca in ppm are: Ba-100, Cd-2500, Mg-100, Na-100, Zn-800, and in the ^{40}Ca: Mg-100, Si-100, and Sr-200. Major impurities in the ^{n}Ca in ppm are: Ba-30, Mg-10, Mn and Sr-5, and Fe, Na, K, Ni, and Si-2. EDS measurements show no impurities in the intercalated samples, although the sensitivity of this technique is not very high.
[21] H. Claus, U. Welp, H. Zheng, L. Chen, A. P. Paulikas, B. W. Veal, K. E. Gray, and G. W. Crabtree, Phys. Rev. B **64**, 144507 (2001).
[22] H. Keller, Struct. Bonding (Berlin) **114**, 143 (2005).
[23] N. Bergeal, V. Dubost, Y. Noat, W. Sacks, D. Roditchev, N. Emery, C. Hérold, J-F. Marêché, P. Lagrange, and G. Loupias, Phys. Rev. Lett. **97**, 077003 (2006).
[24] J. S. Kim, R. K. Kremer, L. Boeri, and F. S. Razavi, Phys. Rev. Lett. **96**, 217002 (2006).
[25] G. Lamura, M. Aurino, G. Cifariello, E. DiGennaro, A. Andreone, N. Emery, C. Herold, J.-F. Mareche, and P. Lagrange, Phys. Rev. Lett. **96**, 107008 (2006).
[26] E. Jobiliong, H. D. Zhou, J. A. Janik, Y.-J. Jo, L. Balicas, J. S. Brooks, and C. R. Wiebe, cond-mat/0604062 (unpublished).
[27] I. I. Mazin, L. Boeri, O. V. Dolgov, A. A. Golubov, G. B. Bachelet, M. Giantomassi, and O. K. Anderson, cond-mat/0606404 (unpublished).
[28] D. G. Hinks, H. Claus, and J. D. Jorgensen, Nature (London) **411**, 457 (2001).